Electric Power from Vertical-Axis Wind Turbines

K. J. Touryan
Flow Industries Inc. and Moriah Research, Denver, Colorado
and
J. H. Strickland and D. E. Berg
Sandia National Laboratories, Albuquerque, New Mexico

Nomenclature

a = interference factor
a_D = downstream interference factor
a_U = upstream interference factor
A = actuator disk area
AR = blade aspect ratio
C = blade chord
C_D = drag coefficient
C_L = lift coefficient
C_n = sine response coefficient
C_p = power coefficient based on wind speed
C_{Pm} = maximum power coefficient based on wind speed
C_R = chord-to-radius ratio
$[C]$ = Coriolis matrix
D_n = cosine response coefficient
F = streamwise force on actuator disk
F_a = vibratory aerodynamic forces
$\bar{F}_a$ = steady aerodynamic forces
F_c = centrifugal forces
F_g = gravitational forces
K = tip speed ratio at which K_{pmax} occurs
K_p = power coefficient based on rotor speed
$K_{p\max}$ = maximum power coefficient based on rotor speed
$[K]$ = stiffness matrix
$\dot{m}$ = mass flow rate through turbine
M = tip speed ratio at which C_{P_m} occurs
$[M]$ = mass matrix
rms = root-mean-square response
R = radius of rotor
$[S]$ = softening matrix
u = structural deflection
U = streamwise velocity at actuator disk
U_D = downstream disk velocity
U_U = upstream disk velocity
U_R = relative fluid velocity in plane of airfoil section
U_W = wind velocity in far wake
U_{WD} = downstream wake velocity
U_{WU} = wake velocity of upwind actuator disk (double streamtube models)
U = freestream velocity
V = local wind speed
V_R = local relative wind speed
V_t = tip velocity
$\dot{w}$ = power output from turbine
α = angle of attack
Γ_B = bound vortex strength
ρ = air density
σ = rotor solidity or stress
Ω = angular velocity of rotor
$1B$ = first butterfly mode
$1F$ = first flatwise mode
$1P_r$ = first propeller mode
$1T$ = first tower mode

I. Introduction

In many places throughout the United States and abroad, wind turbines have evolved into mature, cost-effective energy conversion technologies for converting wind energy to electric power. For example, in 1986, installed wind energy capacity in the United States exceeded 1200 MW, with an estimated electricity output of 600 million kWh. Federal and state solar tax credits and generous allowances for R&D tax shelters provided the major incentives for commercializing wind power in the United States. In spite of some unfortunate misuses of these incentives, a number of high-technology companies were able to improve the performance and reduce the cost of wind turbines in the 50–250-kW range, and are now able to install these turbines at unit costs of $1000/kW or less, for unit cost of electricity below $0.10/kWh, with availabilities better than 95%.

The great majority of these turbines have been the aerodynamically improved versions of the traditional horizontal, propeller-type systems. However, the less well-

Dr. K. J. Touryan is a Sr. Vice President at Flow Industries and Vice President at Moriah Research Company. His research activities are in alternate energy systems, with emphasis on renewable energy technologies. From 1979 to 1981 he was Director of Research at SERI (Solar Energy Research Institute, Golden, CO). Prior to that he was Manager of the Fluid and Thermal Sciences Department at Sandia National Laboratories, Albuquerque (SNLA). Dr. Touryan received his Ph.D. from Princeton University in 1962.

Dr. J. H. Strickland is Member of Technical Staff at SNLA in the Parachute Systems Division. Its research activities are in the areas of unsteady aerodynamics of bluff bodies. From 1973 to 1985 he was Professor of aeronautics at Texas Tech University. He received his Ph.D in 1973 from Southern Methodist University. Prior to 1973, Dr. Strickland worked at Boeing Seattle, GE, Lynn, MA, and at Texas Instruments.

Dr. D. E. Berg is Member of Technical Staff at SNLA in the Wind Energy division. His research interests include the aerodynamics and structural dynamics of wind turbines, with emphasis on vertical axis machines. Prior to that, Dr. Berg worked in Sandia's Experimental Aerodynamics and Aerodynamic Simulation Divisions. He received his Ph.D from California Institute of Technologies in 1977.

Received June 16, 1986; revision received Feb. 12, 1987.

known vertical-axis wind turbine (VAWT) of the Darrieus[1] type (Fig. 1) has undergone considerable engineering development and has gained increased visibility over the past decade. It is now being marketed by at least one high-technology company in the United States.[2]

There are actually several types of vertical-axis turbines (see Sec. II.A), of which two—the Darrieus type and the straight-blade Musgrove turbine[3]—are in the advanced development and commercialization phase. The Darrieus has curved blades that approximate the shape that a perfectly flexible member would assume under the action of centripetal forces, i.e., a shape that minimizes bending stresses. This blade shape is called troposkien (from the Greek for "turning rope"), and the shape is dependent on the turbine rpm. The Musgrove is straight-bladed and can be reefed to provide speed control.

The Darrieus turbine was patented by Darrieus in 1931 and was reinvented by engineers with the National Research Council of Canada in the early 1970s. Sandia National Laboratories built a 5-m-diam research turbine in 1974, followed by a 17-m-diam turbine rated at 60 kW in 1977, and are currently building a 34-m-diam turbine rated at 500 kW. The Canadians built the first large-scale Darrieus turbine rated at 230 kW with an average output of 100 kW on Magdalen Island, Quebec, in May 1977. An unexpected self-start with no brakes destroyed the machine. A major design effort on Darrieus turbines was made by ALCOA with the Department of Energy (DOE) and Sandia technical guidance and support funding. ALCOA built four 17-m, 100-kW units, two of which were grid connected, and one of these was tested successfully for over 10,000 h in storms exceeding 120 mph.[4] ALCOA also tested a 25-m VAWT in 1981, but the machine collapsed when it ran above rated speeds.[5]

From 1977 through 1982, DAF Indal Ltd. (now Indal Technologies Limited) of Ontario, Canada, went through three iterations designing and building 14 50-kW Darrieus turbines. Experience gained with these intermediate-size VAWT's was used to design three 500-kW prototype units, one of which is in operation today. One of these units in Palm Springs (Southern California Edison) is providing a sufficient data base to help optimize future designs. Indal has also developed a wind-diesel test facility in Ontario for stand-alone operation of VAWT's. Indal is continuing development of 500-kW VAWT's and plans to go into production in 1988.

The first fully private sector funded VAWT's in the United States were marketed by FloWind Corporation of Kent, WA, in 1982, and VAWTPOWER of Albuquerque, NM, in 1983. Both turbines were improved versions of the Sandia/ALCOA 17-m turbines. In 1986, FloWind began to market 19-m, 250-kW variable-speed turbines and developed and built two 25-m machines. Some of the 19-m machines are integrated into wind-diesel firm power systems.

The Musgrove variable-geometry vertical-axis turbine was developed by P. Musgrove in the United Kingdom in 1975. The curved blades of the Darrieus are replaced by straight, untapered, untwisted airfoils, and power input is controlled by inclining the blades (see Fig. 2). An industrial consortium formed by Sir Robert McAlpine & Sons Ltd. developed the Musgrove concept using 6- and 25-m designs. Vertical Axis Wind Turbines Ltd. has been formed to continue development of the Musgrove design and commercialize it.

In summary, the two primary advantages a vertical-axis turbine has over the horizontal propeller designs are as follows:

1) Vertical symmetry allows acceptance of variations in wind direction and eliminates the need for yaw mechanisms.

2) The electrical generator, gearbox, brakes, and all major system components are at ground level or attached to the base structure on the ground. This reduces tower requirements and provides for easy maintenance and servicing.

The Darrieus turbine is not self-starting; it relies on the superposition of rotational velocity and incident wind velocity to produce blade lift and generate torque. The nonrotating turbine produces torque only at certain orientations with respect to the incident wind. If the brakes are released, the turbine will simply rotate to an orientation where no torque is produced. The turbine will, however, self-start with the proper type of gusty high winds.

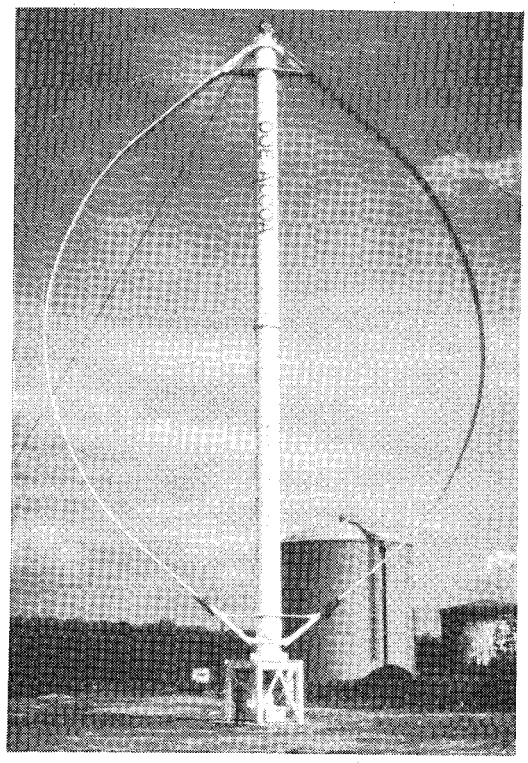

Fig. 1 Typical Darrieus vertical-axis wind turbine.

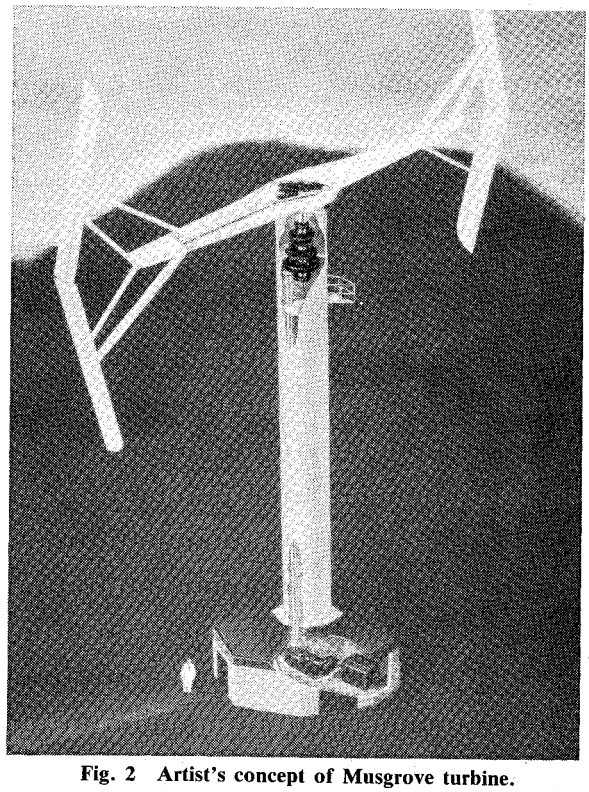

Fig. 2 Artist's concept of Musgrove turbine.

The addition of pitch mechanisms to the turbine could, conceptually, make it self-starting. Pitch control could also be used to regulate power output. However, such a mechanism would have to be capable of producing a wide range of pitch very quickly; the necessary pitch is a function of turbine orientation, not just of rotational speed and incident wind speed as

is the case for horizontal-axis machines. This concept is applied in straight-bladed Giromill designs.[7] In addition, the curved blade would necessitate a very complex mechanical design that would be a maintenance problem. The additional costs far overshadow the potential benefits of such a scheme.

This inability to self-start is not, however, a serious problem. As long as there is another source of power available (i.e., the turbine is connected to the electric grid or is part of a firm power system), the generator may be used as a motor to start the turbine. Once the turbine reaches operating speed, the generator is returned to its conventional power-production role. In the few cases in which the application is truly standalone, auxiliary devices such as Savonius buckets may be attached to the rotor torque tube to start the turbine.

The purpose of this survey article is to critically review the status of the Darrieus-type vertical-axis wind turbine, with emphasis on the aerodynamic, structural, and systems characteristics. To this end, this article is an update of a similar paper, which appeared a decade ago in the *Journal of Energy*.[6] In addition, the article briefly reviews some critical issues involved in making proper estimates for wind resources and their impact on predicting power production from VAWT's, with emphasis on micrositing and array-loss problems.

II. Turbine Aerodynamics

Vertical-axis wind turbines can be classified according to both aerodynamic and mechanical characteristics. By definition, all vertical-axis wind turbines exhibit a common feature in that the aerodynamic lifting surfaces that make up their rotors move about a vertical axis along a path that is usually in a horizontal plane.

A. Aerodynamic Characteristics

There are four types of vertical-axis wind turbines in common use today (Figs. 1-3). These are 1) the troposkien (jump-rope)-shaped fixed-blade Darrieus; 2) the articulating straight-blade Giromill[7]; 3) the variable-geometry Musgrove, which permits reefing of the blades; and 4) the Savonius rotor.[8]

Among the several geometric aspects of VAWT's that can be used to classify them aerodynamically, the most commonly used are: rotor solidity, $\sigma = NCL/A_s$; chord-to-radius ratio, $C_R = C/R$; blade aspect ratio, $AR = C/L$; and the nature of blade fixation with respect to the vertical axis. In these definitions, N is the number of blades, C the chord length, L the blade length, A_s the turbine swept area, and R the maximum turbine radius.

Both the Darrieus and Musgrove turbines are low-solidity ($\sigma < 0.3$), low-chord-to-radius ratio ($C_R < 0.10$), and high-aspect-ratio ($AR > 20$) devices.

Before we discuss the various models depicting the flowfield around VAWT's, a brief description of how the device works is in order here. Figure 4 illustrates the airfoil cross section of the vertical blade. The wind apparent to an observer fixed to the turbine blade is a vector combination of the local wind speed V and the tip velocity V_t ($=\Omega R$). The resulting relative wind velocity V_R acts at an angle of attack a, and creates an aerodynamic force on the airfoil section. This force can be resolved into the conventional lift and drag components, which are strong functions of the local angle of attack a. When the chordwise component of lift exceeds the chordwise component of drag, the aerodynamic torque is positive and the turbine produces power. The net aerodynamic torque of a complete turbine is then determined by integration of the aerodynamic forces along the length of each blade for a full revolution.

B. Aerodynamic Analysis

The aerodynamic analysis of a wind turbine has two objectives: 1) to develop models to predict the aerodynamic performance of the turbine under a variety of wind conditions, which include surface shear, unsteady flow, and stochastic fluctuation; and 2) to use the aerodynamic loads to calculate the structural response of the turbine to wind loads. The results are then used to design the turbine.

Since 1977, significant improvements have been made in the development of multidimensional, quasisteady, and unsteady flow codes to predict the aerodynamic behavior of VAWT's. These can be classified into three categories: 1) momentum methods, which include the streamtube models; 2) vortex methods, which consist of the free-wake and fixed-wake models; and 3) local-circulation methods. In the first method, the flow disturbance produced by the wind machine is determined by equating the aerodynamic forces on the wind turbine rotor to the time rate of change in wind momentum through the rotor using sheets of discrete vorticity. In the second method, the disturbance or perturbation velocities produced by the wind turbine are modeled using sheets of discrete vorticity. The third method utilizes some of the features of both of the other methods. A brief description of each method will be given in the following sections.

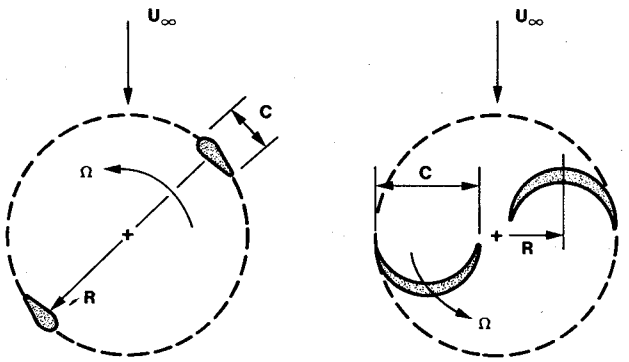

a) Fixed bladed Darrieus or articulating blade Giromill. b) Savonius rotor.

Fig. 3 Types of vertical-axis wind turbines.

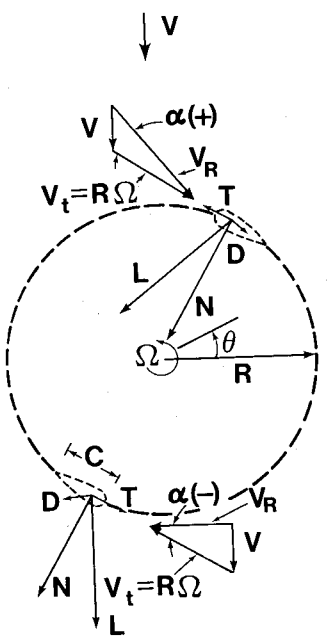

Fig. 4 Relative velocity and aerodynamic forces for typical blade element.

Momentum Models

Momentum models may be classified as single streamtube, multiple streamtube, double streamtube, and double-multiple streamtube. As depicted in Fig. 5, each of the methods listed below assumes that the flow through the rotor can be modeled by examining the flow through one or more streamtubes.

1) Single Streamtube Model: The single streamtube model developed by Templin[9] can be used to form the basis for each of the other variations. This model is based upon equating the streamwise forces on the rotor blades to the change in streamwise wind momentum as the wind passes through the rotor. As can be noted from Figs. 5a and 6a, the rotor is modeled as an "actuator disk" across which a pressure drop occurs equivalent to the streamwise force F on the rotor divided by the actuator disk area A. The power required to slow down the airstream is given by

$$\dot{w} = \dot{m}/2\ (U^2 - U_W^2) \tag{1}$$

where $\dot{m}$ is the mass flow rate through the rotor, and the remaining terms on the right-hand side are the change in kinetic energy per unit mass transfer through the rotor. The power can also be given in terms of the force F on the actuator disk and the disk velocity U as

$$\dot{w} = FU \tag{2}$$

From the momentum principle, the force F is given by

$$F = \dot{m}(U_\infty - U_W) \tag{3}$$

Eliminating F and $\dot{w}$ from Eqs. (1-3), one obtains

$$U = (U_\infty + U_W)/2 \tag{4}$$

which is the classical result that one-half of the velocity defect occurs upstream of the actuator disk and one-half downstream. From Eqs. (3) and (4),

$$F = 2\dot{m}(U_\infty - U) = 2\rho A U(U_\infty - U) \tag{5}$$

where ρ is the fluid density. Equation (5) forms the basis for obtaining the unknown value of U. The streamwise force F can be written in terms of the velocity U given the exact nature of the rotor (i.e., lifting surface geometry and motion). It should be noted that the force F represents the time-averaged force in the streamtube for a complete revolution of the rotor. Equation (5) may, in some cases, be solved explicitly for U, but in most cases it must be solved iteratively.

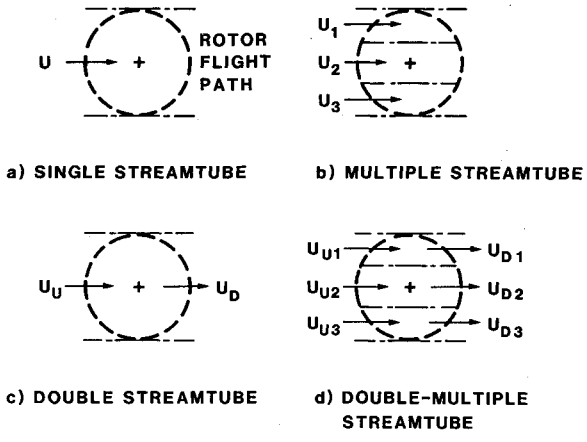

Fig. 5 Streamtube models.

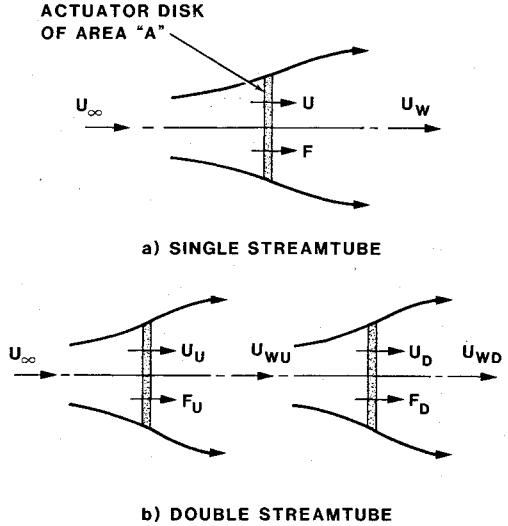

Fig. 6 Single and double actuator disks.

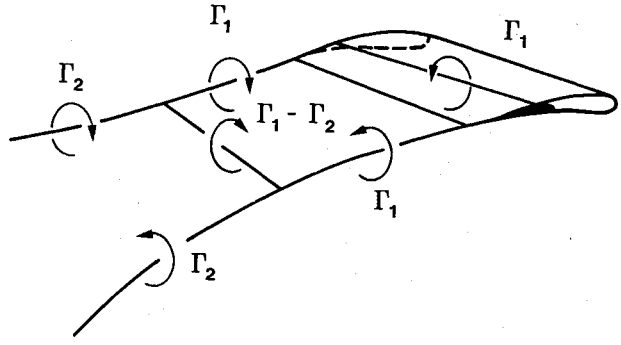

Fig. 7 Vortex system for a single blade element.

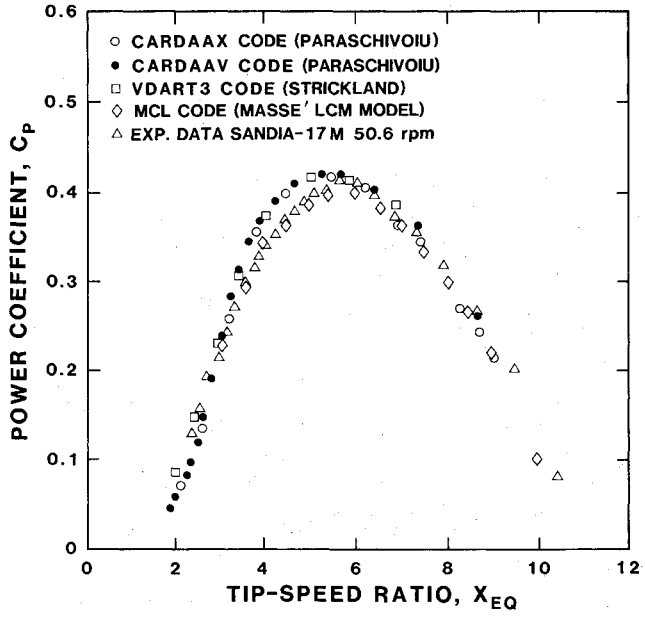

Fig. 8 Performance comparison between theoretical results and experimental data for the Sandia 17-m turbine.[21]

2) Multiple Streamtube Model: The multiple streamtube model, as depicted in Fig. 5b, is simply an extension of the single streamtube model of Templin[9] and has been developed by Wilson et al.,[10] Strickland,[11] and Shankar.[12] Equation (5) is still valid, except that the force F is the time-averaged streamwise force in the local streamtube and the value of U is the fluid velocity in the local streamtube. Wind shear and local Reynolds number effects may be accounted for by using this technique.

3) Double and Double-Multiple Streamtube Models: The double streamtube models depicted in Figs. 5c and 5d make use of a double actuator disk arrangement, as shown in Fig. 6b. These models have been developed by Lapin,[13] Read and Sharpe,[14] Healey,[15] Paraschivoiu,[16,17] and McCoy and Loth.[18] The need for such models arose out of a requirement to determine more accurately the local value of U in the upwind and downwind regions for instantaneous blade-load calculations. In most of the cited studies, it has been assumed that the wake from the upstream region is fully expanded prior to moving into the downstream region. Therefore, the solution of Eq. (5) in the upstream region yields the upwind disk and wake velocities, U_U and U_{WU}. The latter quantity (U_{WU}) provides an input condition for a repeated application of Eq. (5) in the downstream region such that U_D and U_{WD} can be obtained. If interference factors are defined as

$$a = 1 - U/U_\infty;\ a_U = 1 - U_U/U_\infty;\ a_D = 1 - U_D/U_\infty \qquad (6)$$

it can be shown by assuming a fully expanded upstream wake that

$$a_D - a_U = a \qquad (7)$$

that is, the single and double actuator disk theories predict the same total interference. The assumption of a fully expanded wake appears to give reasonable results and, as Healey[15] points out, the problem is indeterminate without some assumption regarding the intermediate wake development. Various methods have been employed to account for the interference factors. For example, McCoy and Loth[18] use a cosine distribution of velocity variation in the lateral direction, which allows calculation at each vertical level using a modified double-multiple streamtube model. Berg[19] incorporated a sine distribution for the induced velocity through the rotor in a double-multiple streamtube model.

Continuing the development of the two-actuator disk theory, Paraschivoiu improved his earlier double-multiple streamtube model by considering the variations in the upwind- and downwind-induced velocities as functions of the azimuthal angle for each streamtube.[20,21] Among the many two-actuator disk models, only the latter includes the influence of all secondary effects, including streamtube-expansion effects, the blade geometry and profile type, the rotating tower, and the presence of struts and aerodynamic spoilers on the Darrieus turbine.

Vortex Models

All vortex models are based upon some form of the vorticity equation. One of the advantages of the vorticity equation is that the pressure does not appear explicitly, allowing one to determine the velocity field without any knowledge of the pressure field. In addition, in many flows, regions of vorticity can be treated as thin sheets or even points of concentrated vorticity, thus greatly facilitating numerical analyses.

Basically, two types of vortex models have been employed to predict the flowfield around vertical-axis machines, although there are a number of variations of these two models. These two types have been referred to as "free-wake" and "fixed-wake" models. The fixed-wake model restricts the motion of the wake in some prescribed manner in order to economize on computational requirements, while the free-wake model places few or no restrictions on the wake motion. In order to illustrate these two methods, the free-wake model due to Strickland et al.[22-24] and the fixed-wake model due to Wilson and Walker[25] will be summarized in the following.

1) Free-Wake Vortex Model: In the free-wake model due to Strickland et al.,[22-24] the general analytical approach requires that the rotor blades be divided into a number of segments along their span. The production, convection, and interaction of vortex systems springing from the individual blade elements are modeled and used to predict the "induced velocity" or "perturbation velocity" at various points in the flowfield. The induced or perturbation velocity at a point is simply the velocity that is superimposed on the undisturbed wind stream by the wind machine. Having obtained the induced velocities, the lift and drag of the blade segment can be obtained using airfoil section data or any other suitable representation of the lifting surface.

A simple representation of the vortex systems associated with a blade element is shown in Fig. 7. The airfoil blade element is replaced by a "bound" vortex filament, sometimes called a "substitution" vortex filament[26] or a "lifting line."[27] The use of a single line vortex to represent an airfoil segment is a simplification of the two-dimensional vortex model of Fanucci and Walters,[28] which uses three to eight bound vortices positioned along the camberline. The use of a single bound vortex represents the flowfield adequately at distances greater than about one chord length from the airfoil. The strengths of the bound vortex and each trailing tip vortex are equal as a consequence of the Kelvin/Helmholtz theorems of vorticity.[29]

As indicated in Fig. 7, the strengths of the shed vortex systems have changed on several occasions. On each of these occasions, a spanwise vortex is shed with strength equal to the change in the bound vortex strength as dictated by Kelvin's theorem.

In order to allow closure of the vortex model, a relationship between the bound vortex strength and the velocity induced at a blade segment must be obtained. A relationship between the lift L per unit span on a blade segment and the bound vortex strength Γ_B is given by the Kutta-Joukowski law.[29] The lift can also be formulated in terms of the airfoil section lift coefficient C_L. Equating these two expressions for lift yields the required relationship between the bound vortex strength and the induced velocity at a particular blade segment:

$$\Gamma_B = \tfrac{1}{2} C_L C U_R \qquad (8)$$

Here the blade chord is denoted by C, and U_R is the local relative velocity of the fluid in the plane of the section.

2) Fixed-Wake Vortex Model: The fixed-wake model of Wilson and Walker[25] follows somewhat along the line of a work by Holme[30] and to some extent a previous development by Wilson[31] concerning the Giromill vortex theory.[32] It should perhaps be noted that Sharpe[33] has also utilized the work by Holme to develop a vortex theory. The method due to Wilson and Walker[25] is a clever combination of vortex theory and momentum theory, in which several assumptions are made to yield a simple method for obtaining the interference factors a_U and a_D. The method is derived for a single streamtube and can be extended to a multiple streamtube version by assuming that each streamtube is independent.

It should be noted that all of the preceding aerodynamic analyses are limited to steady wind inputs *with* surface shear. Efforts are under way to include stochastic wind models in these codes to account for statistical variations in wind speed and direction.

Local Circulation Method

The local circulation model (LCM) is a fairly recent development by Azuma and Kimura[34] and Masse.[35] Similar to the streamtube models, the LCM utilizes a momentum balance between the force on the blade and the change in wind momentum as it passes through the rotor. The blade, however, is represented as a superposition of imaginary blades of different spans with elliptical circulation distributions. The induced velocities due to these imaginary blades may be readily calculated with the Biot-Savart law, and the calculated blade angle-of-attack includes the contribution due to blade-induced velocities. Unlike the streamtube models, which consider the flow as being steady and the streamtubes fixed in time and space, LCM models may be formulated to analyze unsteady flow, and are able to yield detailed flowfield velocity and blade-loading information. The LCM yields better answers than the momentum models, avoids the convergence problems of the vortex models, and, with an appropriate wake model,[37] requires far less computer time than the vortex models. Additional information may be found in the references.

C. Representation of the Airfoil

Proper representation of the lifting surfaces, or airfoils, making up the rotor is essential to obtaining good results from any aerodynamic theory. The lifting surface model chosen will yield the forces required by the momentum models or the circulations required by the vortex models, and must, therefore, adequately represent the lifting surface behavior. Lifting surface models have been constructed from experimental data, linear airfoil theory, and more advanced airfoil theories. Problems related to stall and dynamic effects must also be addressed.

Airfoil Analysis

Two-dimensional airfoil lift and drag data have been widely used to model the lifting surfaces of wind turbines. To date, most Darrieus turbines have used the NACA 0015 airfoil configuration. However, Sheldahl and Klimas[36] have reported test results on seven symmetrical airfoils with angles of attack from 0 to 180 deg. Analytical methods for obtaining lifting surface data range from simple inviscid thin-airfoil theory to nonlinear panel methods. As mentioned previously, Fanucci and Walters[28] represented the airfoil by a series of vortices located along the airfoil chordline. This particular model could not be used to predict C_D, except empirically, and was valid for C_L in the linear and early stall regimes. Eppler and Somers[37] have developed a vortex panel airfoil code, which can be used to calculate both lift and drag coefficients in the linear and early stall regimes.

Dynamic Effects

In most of the preceding cases, analyses are based upon a quasisteady approach. Dynamic effects can become important, however, under certain conditions, and must be accounted for. Unsteady aerodynamic loading of an airfoil can arise due to several effects. In the absence of aerodynamic stall, these effects can be loosely categorized as those due to fluid inertia ("added mass") and those due to unsteady wake circulation ("circulatory lift and moment"). For conditions where boundary-layer separation can occur, a combination of viscous, inertial, and unsteady wake effects give rise to "dynamic stall."

Added mass effects may be readily approximated, but are normally small for the C/R values commonly used on full-scale Darrieus turbines (i.e., $C/R = 0.07$).

The circulatory lift produced by the unsteady wake is automatically included in free-vortex models in an approximate way. The effect of downwash and upwash produced by discrete vortices models this lift. The pitching of the airfoil does require an adjustment in the bound vorticity in order to satisfy the Kutta condition. For small values of C/R, this adjustment is negligible, but at larger values of C/R, this effect must be considered.

These dynamic effects can be approximated for unseparated flows, according to Strickland et al.,[24] by calculating the airfoil thrust coefficient using the angle of attack at midchord and the normal force coefficient using the angle of attack at three-quarter chord. An alternate method for treating these effects is to utilize the "virtual camber" and "virtual incidence" concepts presented by Migliore et al.,[38] in which the airfoil geometry is transformed to account for the curvilinear flowfield.

Inertial effects in the boundary layer and the unsteady wake arising from boundary-layer separation in unsteady flows are often referred to as dynamic stall. These inertial effects produce lift coefficients that may be considerably larger or smaller than the steady-state values. As pointed out by Klimas,[39] dynamic stall results in increased peak aerodynamic torques on the Darrieus turbine. This effect significantly impacts the drive-train/ generator sizing and system reliability. Dynamic stall is a highly complex problem, but has been approximated with a fair amount of success in some cases[40] using a modified Gormont or Boeing-Vertol method.[41] A summary of dynamic stall effects on wind turbines is presented by Noll and Ham.[42] Oler et al.[43] have recently developed a vortex panel method utilizing discrete vortices and turbulent boundary layers to model separating wakes and to predict the aerodynamic characteristics for unsteady airfoil motion at high angles of attack ($\alpha \approx 60$ deg). At present, only the steady, attached-flow version of this code is accurate enough to be used as an analysis tool.

D. Comparisons Between Theory and Experiment

Experimental data for Darrieus turbines are available for the Sandia 17-m,[4,44] FlowWind 19-m, and Indal 500-kW systems. These include both wind-tunnel tests and field tests with full-scale prototypes.

To compare the various aerodynamic models with experimental data, a performance curve (power coefficient vs blade tip-speed ratio) and several force data (normal and tangential) have been selected. In Fig. 8, CARDAAV and CARDAAX are Paraschivoiu's double-multiple streamtube codes[20,21] (CARDAAX contains lateral streamtube expansion effects), VDART3 is Strickland's three-dimensional free-wake code,[22] and MCL is Masse's local circulation method code.[35] As seen in Fig. 8, the double-multiple streamtube, local circulation method, and three-dimensional free-vortex models all agree fairly well with the experimental data from the Sandia 17-m turbine at all wind speeds, including the low tip speed ratios where dynamic stall effects are largest. For this set of experimental data (50.6 rpm), no comparison is available with Wilson and Walker's fixed-wake theory.[25] However, a comparison available at 42.2 rpm shows equally good agreement with the fixed-wake theory.

The importance of including dynamic effects becomes evident when comparing the preceding theories with tangential and normal blade force data, as in Fig. 9 where the free-wake models (both quasisteady and dynamic) are compared with data taken in tow tanks.

Although comparisons of all of the preceding theories with blade force field-test data are not available at present, it is clear that the double-multiple streamtube models and the fixed-wake vortex model are better representations of the physical phenomena than the simpler streamtube models, and thus would be expected to yield *instantaneous* blade force predictions superior to those predicted by the other streamtube models. All of these models are relatively inexpensive to run in terms of computer time. The free-wake vortex model is the most physically realistic model and yields very good predictions of rotor performance, blade forces, and wake velocities. The computer time required for the two-dimensional case is moderate, while that for the three-

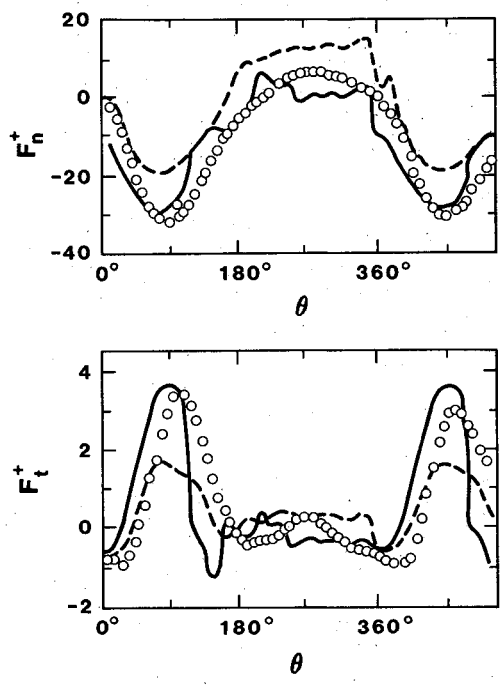

Fig. 9 Blade force data for a two-dimensional rotor ($Re = 40{,}000$, two blades, $U_T U_\infty = 5.0$: •, tow tank data; — — —, quasisteady model; ____, dynamic model).[24]

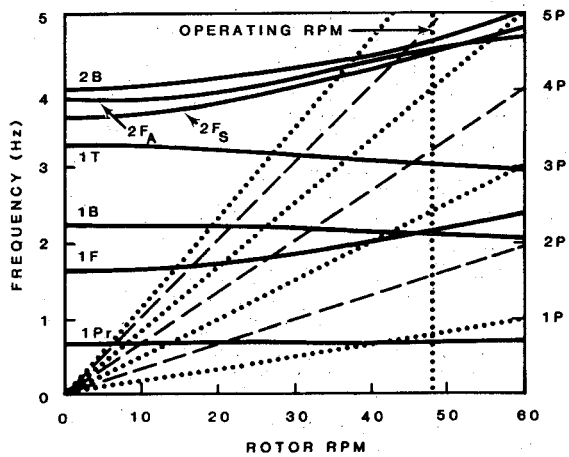

Fig. 10 Fan plot and system driving frequencies for the Sandia/DOE 100-kW turbine.

dimensional case is large. All of the models should include dynamic effects for best results.

III. Structural Dynamics

Both Canadian and U.S. Darrieus turbine designs use relatively slender, high-aspect-ratio structural elements for the blades and supporting tower. These design efforts have underscored the importance of developing a relatively complete and accurate understanding of the structural dynamics of VAWT's. In addition, structural constraints have become an integral part of aerodynamic requirements in all design optimization efforts of present-day Darrieus turbines.

The critical structural dynamic problems for VAWT's concern the response of the rotor to cyclic loads that are dominated by loads at the harmonics of the basic rotational speed. These structural problems may be categorized into three main topics:

1) Response to nominal loads. The three major loading cases are: a) combined aerodynamic and gravitational loads on the blades for the parked rotor subjected to high winds; b) combined aerodynamic, gravitational, and centrifugal loads on the blades during normal rotor operation; and c) combined aerodynamic, blade, cable, and gravitational loads on the rotor tube for the parked rotor subjected to high winds.

2) Material structural properties. The most critical areas here are: a) blade-joint fatigue characteristics, b) system resonant frequencies, and c) critical buckling loads of the blades and rotor tube.

3) Response at resonant conditions. The critical issues here are the structural responses due to a) aerodynamic excitation at integer multiples of the rotating frequency, b) aerodynamic excitation caused by the stochastic nature of the wind, c) aerodynamic excitation due to the shedding of vortices from the tower and the impingement of those vortices on the downstream blade, and d) aeroelastic excitation due to flutter instability.

As discussed by Blackwell et al.[6] in 1976, the structural design of the turbine support system, namely the tower and the guy cables, can proceed along more conventional lines than can the design of the blades. The most obvious reason for this is the relaxation of the aerodynamic constraints. Consequently, linear beam theories,[45] linear finite-element analyses,[46] and conventional guy-cable analyses have been the principal tools in tower, base, and tiedown design. These analyses have led to a simple tubular torque tube (or tower) design with substantial factors of safety and a dual guy-wire system (see Sec. IV).

There are several features of the structural evaluation of wind turbine blades, however, that should be addressed in dynamic analysis. These include: the determination of turbine rotor modes and frequencies of vibration, identification of aeroelastic instabilities, and prediction of the amplitudes of rotor response to fluctuating wind loads. The first two of these design issues have been the focus of relatively detailed theoretical and experimental efforts.[45-52] Only very recently have issues regarding fluctuating or stochastic winds been included in Darrieus turbine design studies.[53]

A. Frequencies, Mode Shapes, and Response Levels

Finite-element structural programs capable of solving eigenvalue problems are well suited for frequency and mode-shape analysis because of the analytically complex shape of the turbine blades. The development efforts for these numerical codes have focused on the derivations of mass, damping and stiffness matrices, and force vectors appropriate to the VAWT.

Finite-Element Codes

Two finite-element codes are in common use today: a natural-frequency analysis code (FEVD)[51,52] and a forced-vibrational-response analysis code (FFEVD),[54] both used in conjunction with the general-purpose finite-element NASTRAN code[55] to provide the system's natural frequencies and mode shapes. The equations of motion are developed in a coordinate system that rotates with the turbine at its angular velocity. Because the VAWT support system consists of guy wires (cables) with mass much smaller than the mass of the rotating components, and because the stiffness of the guy cables in the plane parallel to the ground is essentially independent of the rotational angle, the total turbine system can be modeled in the rotating coordinate frame with time-independent coefficients. For small motions, u, relative to the rotating frame, the finite-element equations of motion may be represented by[49,51]

$$[M]\{\ddot{u}\} + [C]\{\dot{u}\} - [S]\{u\} + [K_r]\{u\} = \{F_c\} + \{F_g\} + \{F_a\} \tag{9}$$

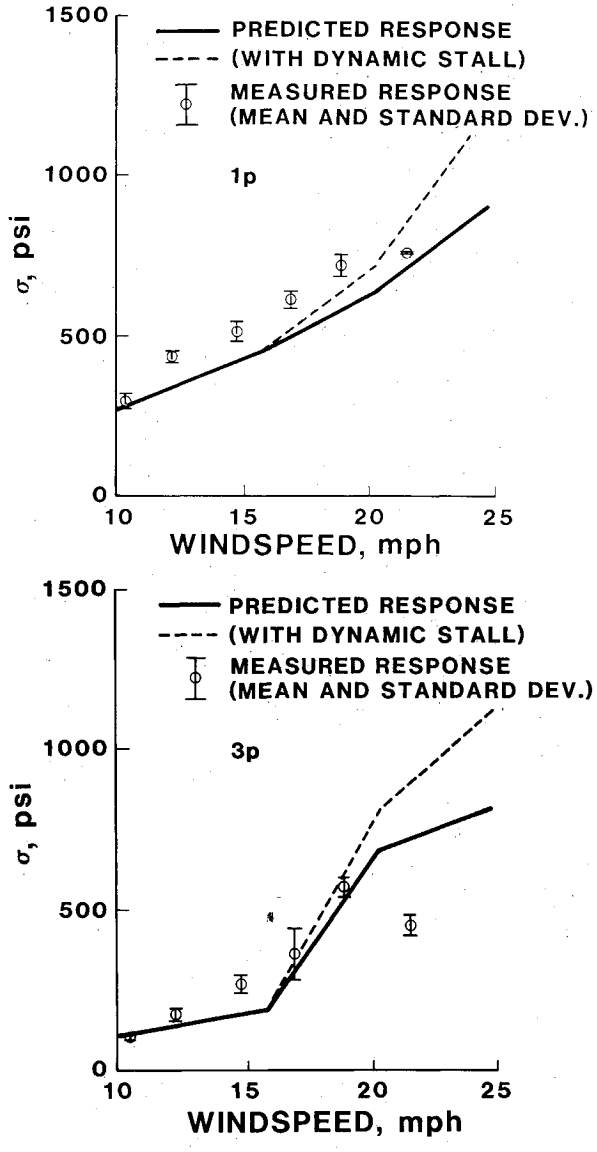

Fig. 11 Measured and predicted 1P and 3P longitudinal stresses at blade leading edge.[48]

The first two terms on the right-hand side are the steady centrifugal and gravitational forces, while the third is the aerodynamic force, which contains both steady and oscillatory components. $[M]$ and $[K_r]$ are the mass and the revised stiffness matrices, and $[C]$ and $[S]$ are the Coriolis and softening matrices, respectively (the softening matrix accounts for changes in the centrifugal force that result from the structural deformations). $[K_r]$ is the solution of

$$[K_r(u)]\{u\} = [S]\{u\} + \{F_c\} + \{F_g\} + \{\bar{F}_a\} \qquad (9b)$$

where $\{\bar{F}_a\}$ denotes the steady component of the aerodynamic loads. Results from computations using $[K_r]$ represent deformation from a state in which the turbine is prestressed by gravitational, centrifugal, and steady aerodynamic loads.

To obtain the modal characteristics of the rotor rotating at a specified angular velocity, the right-hand side of Eq. (9a) is set to zero. The frequency response of the rotor driven by the oscillatory aerodynamic loads is found by solving the following equation in the frequency domain:

$$[M]\{\ddot{u}\} + [C]\{\dot{u}\} - [S]\{u\} + [K_r]\{u\} = \{F_a\} \qquad (10)$$

The oscillatory aerodynamic forces $\{F_a\}$ for *steady* wind conditions are computed using either a double-multiple streamtube model[17] with dynamic stall and variable Reynolds number effects or a much simpler single streamtube aerodynamic model[9] (see Sec. II). These forces are then Fourier decomposed into the contributions due to the integral multiples of rotor rotational frequency.[47]

This procedure yields frequency-response results in the form of sine and cosine response coefficients (C_n and D_n, respectively) for each of the multiples of rotation frequency or per revolution excitation. To compare these values with vibratory test data, the rms value is computed from

$$\text{rms} = [\Sigma(C_n^2 + D_n^2)/2]^{1/2} \qquad (11)$$

and compared with the rms test data.

The variation of the rotor response with rotor rpm may be calculated and then exhibited on "fan plots" (see Fig. 10). Also presented on the plot are multiples of the turbine rpm—the driving frequencies. The intersection of these per-rev frequencies (P) and the natural rotor frequencies show where resonance problems could occur. Only a few of the lower frequency, more important modes are plotted in Fig. 10, where 1F is the first flatwise (symmetric and asymmetric) mode, $1P_r$ the first propeller mode, 1B the first butterfly mode, 1T the first tower mode, etc. These mode names refer to the appearance of particular modes at 0 rpm. Not all of the intersections shown result in significant resonances, however. Only the lower system driving frequencies (4P or below) contain sufficient energy, in general, to excite a resonant condition, and each turbine mode will only be driven by certain harmonics. For example, for a two-bladed rotor, the first tower (1T) mode will not couple with the even driving frequencies (2P or 4P). The mode intersections of major concern (because they are potentially catastrophic) are 1B/1P, 1T/3P, and 1F/2P. Other intersections that may cause problems but are probably not catastrophic are 1F/3P and 1B/3P.

Typical Measured and Predicted Results

Figure 11 shows samples of both predicted and measured responses from the Indal 6400 VAWT (500 kW) installed at Southern California Edison's test site at Devers, CA.[48] The nominal rotor speed was 45 rpm. Only the 1P and 3P responses are presented, because experience has shown that these harmonics are associated with the greatest response of the rotor. The measured data are the longitudinal stresses in the blade obtained from strain gages located at the leading edge of the blade, reduced using the Method of Bins.[56,57] The lines indicate predicted stresses, with and without dynamic stall, while the circles and bands indicate the mean and standard deviation of the binned measurements. When dynamic stall is included, the measured 1P responses exceed the predicted values, whereas at 3P the reverse is true. This may be due, in part, to errors in the structural modeling of the turbine (the fundamental rotor natural frequency is predicted at 1.08 Hz but measured closer to 1.00 Hz). Including aerodynamic damping in the model will reduce the predicted values.

The preceding results are part of a structural response evaluation conducted by Malcolm[48] on the Indal 500-kW VAWT over a full range of wind speeds in order to obtain a more complete comparison between theory and experiment. The Indal results, plus those obtained by Lobitz and Sullivan[47] on the DOE 100-kW turbine, show that the FFEVD code, with the double-multiple streamtube analysis, provides reasonable predictions for turbine response to centrifugal, gravity, and aerodynamic loads. Inserting the effect of dynamic stall into the aerodynamic model increases the predicted structural response at all locations and frequencies for wind speeds greater than 16 m/s (35 mph). Although the

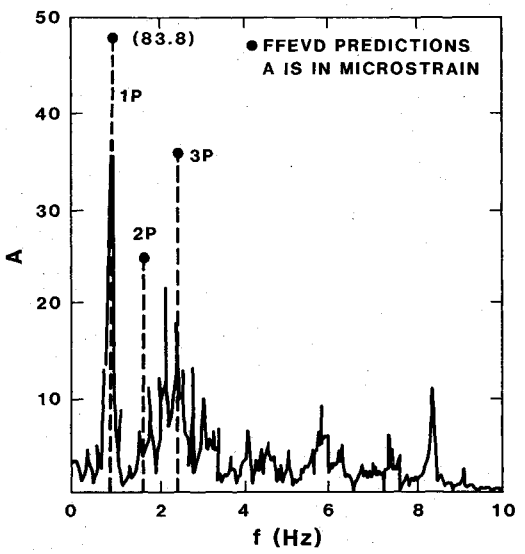

Fig. 12 Amplitude spectrum for upper leading-edge gage, 30-mph winds (Sandia/DOE 100-kW turbine).[47]

values predicted using dynamic stall are in better agreement with field data than those without dynamic stall, the rate of increase of stresses with wind speed is not well predicted.

B. Aeroelastic Effects

Aeroelastic phenomena give rise to two major VAWT structural dynamic effects. First, the aerodynamic loads may couple with the blades to increase their motion, a potentially fatal condition known as flutter instability. Second, the aerodynamic loads may interact with the blades to decrease their motion, a beneficial condition known as aerodynamic damping.

Although the aeroelastic analyses of wind turbines is entirely analogous to that of the wing structures of subsonic aircraft, aeroelastic effects for VAWT's have been addressed only recently,[49,50] mainly because predicted flutter speeds tend to be two to three times greater than turbine operating speeds. Aerodynamic damping, on the other hand, can significantly reduce the flatwise blade oscillation, especially near resonance, lowering the predicted rms peak stress by as much as 20%.

The most recent VAWT analysis that includes aeroelastic effects is by Lobitz and Ashwill[50] for the Sandia 34-m design. They use a specially designed preprocessor (FFEVD) for the NASTRAN code, where the damping and stiffness matrices are appropriately modified for aeroelastic effects and calculations are obtained for either natural frequency or forced response of the VAWT. Although the inclusion of aerodynamic damping in the FFEVD code does create some additional complexity, the basic structure of the package is not altered.

It is important to note here that the use of the preceding structural dynamic analyses and experimentation has led to important rotor design modifications, which include a better approximation of the true troposkien shape for the blades,[58] reduction of motor component weight, and the use of shallow rigid blade-to-tower struts to improve the turbine structural integrity while minimizing any adverse effects on the turbine aerodynamic performance.

C. Fluctuating Wind Loads

At this point in time, both aerodynamic and structural dynamic analyses have been carried out using a steady incident wind with shear. Wind, however, is stochastic in nature, with significant variations in both direction and velocity. In addition, as turbines become larger the relative size of an atmospheric gust or eddy becomes smaller than the size of the turbine and the effect of a stochastic wind becomes greater. Lobitz[54] and Connell[59] point out that the aerodynamic codes discussed in Sec. II must be modified to account for the effect of wind fluctuations on aerodynamic loads, and the effect of these fluctuations on the turbine stresses must be evaluated. In fact, examination of the response spectra clearly shows that atmospheric turbulence induces a broadband response in the 100-kW VAWT (see Fig. 12, for example). Sandia has initiated a significant effort aimed at modifying both aerodynamic and structural dynamic codes to incorporate stochastic-wind models. However, a good space- and time-resolved multipoint description of turbulence velocities that is economical and accurate is still needed to provide input data for these codes.

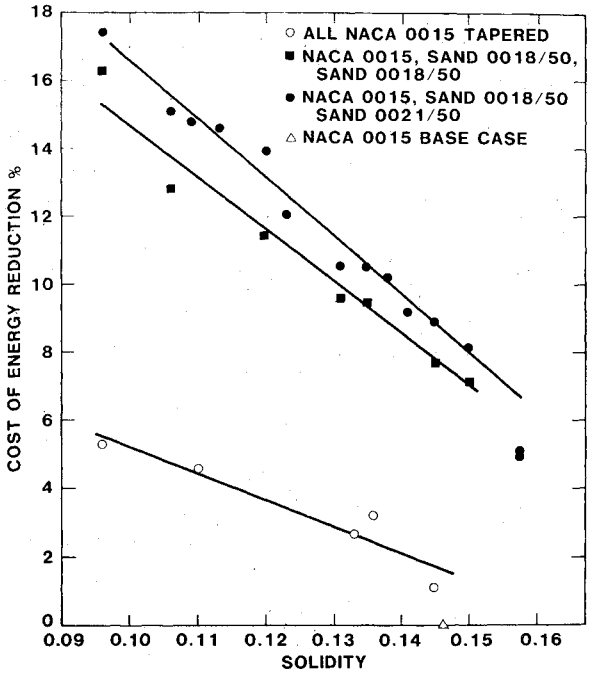

Fig. 13 Predicted Cost Reductions

IV. Systems Engineering

In the preceding sections, improvements over the past decade in aerodynamics and structural dynamic analyses of vertical-axis wind turbines have been discussed. It is clear from these discussions that a number of design parameters are available in each area that can be utilized by wind turbine designers to extract optimum amounts of energy from the wind and ensure structural integrity. The purpose of systems engineering efforts is to achieve overall system design goals for VAWT's by providing both cost and performance assessments for these turbines.

Operating experience over the past decade has demonstrated that the Darrieus turbine is well suited for midrange operation (100–600 kW) at constant speed, tied into a synchronous utility grid for electric power generation. Over the past six years, extensive performance data have been obtained on three midrange turbines: the DOE and FloWind 17-m, 120-kW systems; the FloWind 19-m, 250-kW system; and the Indal 26-m, 500-kW system. These data have been collected for a wide range of wind speeds (exceeding 120 mph), at a variety of geographic locations, and from turbines operating as single units and in multiple-unit wind farms.

This operational experience has provided a reliable database, which will be very valuable in the design, development, and commercial use of future Darrieus machines. Questions regarding component cost estimates, preferred

Table 1 Specifications for operational VAWT's

	DOE/FloWind 17-m	FloWind 19-m	Indal 26-m
Peak output, kW	120/150	250	500
Wind speed peak output, m/s (mph)	18/20 (40/45)	20 (45)	20 (45)
Cut-in wind speed, m/s (mph)	4.8 (10.5)	3.5 (7.5)	6.3 (14)
Cut-out wind speed, m/s (mph)	27 (60)	27 (60)	25 (54)
Rotor rpm	48.1/53	52	45
Rotor diameter, m (ft)	17 (56)	19 (62)	26 (85)
Total height, m (ft)	29 (92)	31 (102)	44 (135)
Total weight, kg (lb)	13,000 (29,000)	20,000 (44,000)	40,000 (90,000)
No. of blades	2	2	2
Blade section	NACA 0015	NACA 0015	NACA 0018
Blade chord, m (in.)	0.6 (24)	0.7 (28)	0.7 (29)
Tower tube diameter, m (in.)	0.91 (36)	1.06 (42)	Tapered: Center 2.4 m/5 ft Root 1.0 m/3 ft
Guy cables	6 (3 sets of 2)	6 (3 sets of 2)	6 (3 sets of 2)

fabrication techniques, turbine installation procedures, utility interconnection requirements, control and safety subsystem requirements, and special requirements for principal markets may all be answered more promptly and accurately with the help of this database.

A. Existing Turbine Systems

Table 1 lists the performance specifications and physical characteristics of the three midrange turbine systems mentioned previously that are in an advanced prototype development stage and/or in production.

B. System Design Guidelines

Analysis of data from these three VAWT's along with detailed systems engineering studies has led to a number of system design guidelines that have been incorporated in the 19-m FloWind turbine, the 500-kW Indal turbine, and other new-generation turbines. These guidelines are summarized below.

1) Design Optimization Criteria[6]—System optimization studies have been based on minimizing cost per unit energy ($/kWh). This cost criterion is more useful than the criteria of $/M^2 of swept area or $/installed kW and is suggested by utilization of wind energy systems in a fuel-saver role. The worth of wind energy systems to a utility, however, will involve other considerations, such as the time history of energy output in relationship to load demand (peaking power vs base load) and time off line due to insufficient winds. Presently, detailed optimization studies for VAWT's consist of cost reduction estimates: first, as a function of aerodynamic performance; second, as a function of the VAWT structural integrity; and finally, as a function of the power conversion equipment (including controls and safety considerations). Table 2 provides a typical cost breakdown among the various components or subsystems of VAWT's. These percentages continue to change as new manufacturing techniques are introduced and VAWT's enter the mass-production phase.

2) Aerodynamic Design Goals—A recent Electric Power Research Institute study[60] investigated the effects on cost of energy of modifying VAWT aerodynamic parameters. The study concluded that significant cost of energy reductions could be achieved by a) increasing the maximum power coefficient C_{P_m}; b) moving the tip speed ratio K associated with stall regulation $K_{p\max}$ closer to the tip speed ratio M of the maximum power coefficient C_{P_m}, i.e., K/M approaching 1; and c) moving the power coefficient curve to higher tip speed ratios. Detailed calculations[61] show that a proper combination of the NACA 0015 low-drag, late-stalling airfoils with the natural laminar flow (NLF), low-drag, early-stalling airfoils does produce the preceding desired effects.

The actual technique of achieving this combination is to use tapered blade geometries that have a larger chord at the root of the blade and a shorter chord at the equator. In one design, this taper is *continuous* using a NACA 0015 airfoil made of fiberglass composites. In another design, the taper is in steps, starting with a larger chord NACA airfoil at the blade root, followed by a smaller chord SAND NLF airfoil in the intermediate section of the blade, followed by a second and shorter chord NLF airfoil at the equatorial section of the blade. Figure 13 illustrates the predicted cost reduction effect of this type of configuration. Under optimum conditions, the reduction in cost of energy can be as high as 17% compared to the base NACA chord 0015 constant chord blade. The new Sandia 34-m, 500 kW VAWT, which is a research machine, will have aluminum blades with such a three-step tapered configuration.[62]

3) System Configuration—Another cost reduction scheme for the new-generation VAWT's is to use either a multiple constant-speed design (i.e., capable of operating at any of several selectable constant rotational speeds) or a continuously variable speed design. This will enable the VAWT to take advantage of lower cut-in wind speeds and still operate efficiently at higher wind speeds, thus increasing energy capture. The multiple constant-speed approach has given present-day horizontal-axis turbines a higher energy capture characteristic at low average wind speeds (12–16 mph). The FloWind 19-m turbine uses a low-speed induction generator (see Table 1) to lower its cut-in wind speed and thus increase annual energy capture for a given site by 5%. The new Sandia 34-m VAWT will employ a continuously variable speed generator to provide a turbine operating range of 25–40 rpm.

4) Structural Design Goals—Once the blade configuration has been selected using aerodynamic analyses, the FEVD and FFEVD vibrational frequency and structural response analysis codes are used to evaluate the structural dynamics of the aerodynamically "optimized" system. An iterative procedure is usually required to determine a combination of

Table 2 Relative cost breakdown of VAWT components (FloWind 19-m turbine)

Components	Cost, % of total
Rotor assembly[a]	37
Guy cable assembly	5
Drive train assembly	18
Controller assembly	19
Base structure assembly	21

[a]The blades themselves constitute 43% of the rotor assembly or 16% of the entire turbine.

tower stiffness, blade-to-blade and blade-to-tower joints and strut configuration that will result in acceptable stress levels. Berg[62] describes, in some detail, the preceding design process in selecting the final configuration for the Sandia 34-m, 500-kW Darrieus turbine. The design has evolved into a machine with a rotor height-to-diameter ratio of 1.25 and a blade that has a 1.22-m (48-in.)-chord NACA 0021 profile at the root, a 1.07-m (42-in.)-chord SAND 0018/50 profile in the intermediate section, and a 0.91-m (36-in.) SAND 0018/50 profile at the equator. The turbine has a very stiff tower design, rigid tower-to-blade joints, slope discontinuities at the blade-to-blade joints, and no struts.

5) Power Conversion Equipment—With the aerodynamic and structural design process complete, attention is focused on the power conversion equipment, which includes the gearbox and drive train, the induction generator, the control system, the bearing assembly, and the brake system. It is not possible to discuss the various features of these components in this survey article. The reader may refer to Refs. 4, 61, and 62 for details. It is important to note, however, that good control features and a highly reliable brake system are crucial elements in the longevity of the VAWT design. The turbines should have automatic high-wind shutdown controls, independent overspeed controls, and phase-loss and voltage-level sensors to provide a shutdown signal should there be a utility line loss or low control system voltage. Finally, most VAWT's employ three independent sets of brake calipers, two as service brakes (used alternately) and one for parking. The brakes are typically placed on the low-speed side of the power train to minimize loading of the transmission and to maximize braking reliability.

6) System Reliability and Life—Studies made of wind energy systems between 25 and 250 kW in size indicate that the component failure rate is between one and six failures per year per turbine, reducing the nominal average operating time to 4500 h/yr.

A 30-year life is often considered to be a realistic goal for the wind turbine rotating and support structures. This goal can readily be met for the support structure in which the design conditions are well established. Lifetimes of these structures can be reasonably well predicted. This 30-year life goal is not as well met for the rotating structure, in large part because the lifetime of a given rotor cannot be adequately predicted. The lifetimes of off-the-shelf components are, in many cases, well known, and detailed fatigue and structural testing of the components and the improvement of structural and fatigue models have led to a better understanding of the rotor blade's response and fatigue characteristics. The primary obstacle remains the fact that the operating environment is not adequately characterized—the stochastic-wind-induced effects may well be the limiting factors in rotor life.

V. The Future: Concluding Remarks

At current energy prices and in the absence of tax credits, wind-generated electric power is only marginally competitive from an economic standpoint. Only in Alaska and at remote sites far from major electricity transmission lines is wind power truly competitive.

A. Cost Estimates

At present, conservative estimates for the cost per unit energy for VAWT's are about \$0.50/*annual* kWh, which, when amortized over a 10-year period, would translate into \$0.06–0.09/kWh, depending on interest rates and inflation figures. Therefore, a "reasonable" levelized cost goal would be approximately \$0.06/kWh in 1990. Turnkey costs have to be \$500 to \$800/kW. To this one should add the operation and maintenance (O&M) costs. The latter has been decreasing as the machine size has increased, and now ranges between 10 and 20% of the cost per unit energy.

The most promising developments for VAWT's, however, lie not in the size of the machine, but in the development of effective and inexpensive construction procedures as well as "simple and cheap" subsystems. Today, most VAWT blades are made of extruded aluminum. The Canadian 4-MW Eole turbine[63] utilizes box construction steel blades with a chord of 2.4 m. Future blade designs may well include fiber-reinforced plastics (or composites).

B. Micrositing and Array Losses

Wind farms today generate over 90% of the wind-generated electric power (1200 MW in 1986) in the United States. Most of these wind farms are located in "windy" mountain passes, such as Altamont Pass east of Oakland, CA; Tehachapi Pass near Bakersfield, CA; and San Gorgonio Pass near Palm Springs, CA. These are *complex terrains* where fluctuations in wind speed over relatively small distances (50–100 m) can yield significant variations in energy generation. For example, the entire Altamont area is in the same general wind flow regime during the hours of 1200 to 1900 Pacific Daylight Time when maximum temperature and atmospheric instabilities occur in the general area. During this period, hourly-average wind speeds for sites 50–100 m apart can differ by more than 3.5 m/s. This wind speed variability is due mainly to localized wind flow phenomena such as negative vertical wind shear.

There is a definite need for a predictive tool that can utilize micrometerological modeling to help discriminate clearly between suitable and unsuitable sites. Some numerical models do exist for three-dimensional flowfield analysis of microsites, but they are very sensitive to input parameters such as number of wind observations, details of terrain features, and atmospheric boundary-layer stability.

Examples of recent attempts at improving micrometeorological models are those of Kitade et al.[64] and Barnard et al.[65] The latter utilize a mass-consistent numerical flow model using a single-variable, unconstrained optimization procedure that adjusts the unknown parameters such that the error between the observed winds and model calculations of these winds is minimized. These models need continued experimental verification over a wide range of wind speeds and topographies to improve their usefulness.

Wake interference among machine arrays represents another unsolved problem. The common practice today is to separate adjacent turbines by three turbine diameters and use a downstream spacing between rows of eight turbine diameters. Interference problems between adjacent turbines have been examined by Schatzle et al.[66] Although energy recovery in a turbine wake can be estimated reasonably well, the effect of turbulence of the upstream VAWT on the downstream VAWT could be detrimental, and is not well understood. Indications are that *downstream* VAWT arrays suffer fatigue failure earlier than upstream arrays. A DOE-sponsored project is under way to quantify this wake interference issue.

C. Market Penetration

A large momentum was imparted to the growth of solar technologies in general, and wind power in particular, by the federal government. This support came from increased R&D funding, favorable tax credits for domestic and industrial use of solar energy, and tax shelters for high-risk R&D ventures.

A detailed study by the Energy System Program Group of the International Institute for Applied System Analysis in Vienna[67] showed that *time* was the main factor limiting the full development of a new energy system such as wind power. Public and private support can advance development up to the point of prototype and demonstration plants; thereafter, a different set of factors is responsible for allowing a new energy technology to take over and replace an older, established one.

In particular, Marchetti and Nakicenovic[67] have discovered a regular pattern in the substitution of one energy source for another over decades. Employing available data on the use of various primary energy forms, such as wood, coal, oil, natural gas, and nuclear energy, they found that the penetration of a given energy technology starts with a build-up rate that is exponential as it grows from 1 to 10% of the market it serves. For global systems, the "takeover" time (or 50% penetration of the technology) is 100 years. For smaller systems, this market penetration is shorter, say 40–50 years. Based on these observed patterns, for example, by the year 2000 we might expect a share for solar energy in the United States of 7–8%.

This constraint has some important implications for public- and private-sector planning and leads to the following observations[68]:

1) Sustained long-range plans are essential for the eventual market penetration of solar technologies, and these plans can be provided only by the federal government. The private sectors expect return on their investments in three years, not 20.

2) The free market *will not* voluntarily tie up capital in alternate energy sources, including renewables, in view of competing, *unstable* oil/gas prices.

What the future will bring in a government subsidies-free market where competing oil prices remain highly unstable is not clear. At present (early 1987), market penetration in the utilization of wind power is too low (less than 1%) to allow one to predict the build-up rate observed by Marchetti et al. for competing energy technologies. It is hoped, however, that the steady decrease in the cost of wind turbine systems resulting from the experience gained by four years of continuous operation with wind farms will help the wind power industry maintain enough momentum to compete with the established fossil-fuel technologies.

VI. Summary

Significant advances have been made in vertical-axis wind turbine (VAWT) technology in the 10 years since the last survey article on the Darrieus VAWT appeared in the *Journal of Energy*. At that time, the Darrieus was a new concept and very little was really known about it. Aerodynamic and structural analysis tools were virtually nonexistent, and only a couple of research machines existed. We now have well-proven aerodynamic and structural analytical codes that yield good agreement between theory and experiment for mean aerodynamic and structural characteristics of these VAWT's. Machines are being built by at least three companies: one in the United States, one in Canada, and one in the United Kingdom, and over 550 are in service in California wind farms. The main areas in which better analytical tools are required deal with stochastic wind and aerodynamic effects modeling and better fatigue life predictions.

Acknowledgment

This work was supported by the U.S. Department of Energy under Contract DE-AC04-76DP00789.

References

[1]Darrieus, F.M., *Turbine Having its Rotating Shaft Transverse to the Flow of Current,* U.S. Patent 1,834,018, Dec. 8, 1931.

[2]Vas, I.E. and Watson, R.A., "Engineering and Performance Review of the Cameron Ridge Wind Farm Using the FloWind Turbines," FloWind Corp., Pleasanton, CA, EDF 60050, April 1985.

[3]Clare, R. and Mays, I.D., "The Musgrove Variable Geometry Vertical-Axis Wind Turbine," *Modern Power Systems,* Dec. 1982.

[4]Nellums, R.O., "Field Test Report of the DOE 100 kW Vertical Axis Wind Turbine," Sandia National Laboratories, Albuquerque, NM, SAND84-0941, Feb. 1986.

[5]Townsend, F.M. and Folkenburg, R.J., "Alcoa ALVAWT Program," *Proceedings of Fifth Biennial Wind Energy Conference and Workshop,* Vol. I, SERI/CP-635-1340, Oct. 1981, pp. 311–330.

[6]Blackwell, B.F., Sullivan, W.N., Reuter, R.C., and Banas, J.F., "Engineering Development Status of the Darrieus Wind Turbine," *Journal of Energy,* Vol. 1, Jan. 1977, pp. 50–65.

[7]McConnell, R.D., "Giromill Overview," *Proceedings of Wind Energy Innovative Systems Conference,* SERI/TP-245-184, May 1979, pp. 319–333.

[8]Savonius, S.J., "S-Rotor and Its Applications," *Mechanical Engineering,* Vol. 53, May 1931, pp. 333–338.

[9]Templin, R.J., "Aerodynamic Performance Theory for the NRC Vertical-Axis Wind Turbine," National Research Council of Canada, Ottawa, Ontario, Canada, LTR-LA-160, June 1974.

[10]Wilson, R.E., Lissaman, P.B.S., and Walker, S.N., "Aerodynamic Performance of Wind Turbines," Department of Mechanical Engineering, Oregon State University, Corvallis, OR, ERDA/NSF/04014-76/1, June 1976.

[11]Strickland, J.H., "The Darrieus Turbine: A Performance Prediction Model Using Multiple Streamtubes," Sandia National Laboratories, Albuquerque, NM, SAND75-0431, Oct. 1975.

[12]Shankar, P.N., "On the Aerodynamic Performance of a Class of Vertical Shaft Windmills," *Proceedings of the Royal Society of London,* Ser. A, No. 349, 1976, pp. 35–51.

[13]Lapin, E.E., "Theoretical Performance of Vertical Axis Wind Turbines," ASME Paper 75WA/ENER-1, Dec. 1975.

[14]Read, S. and Sharpe, D.J., "An Extended Multiple Streamtube Theory for Vertical Axis Wind Turbines," *Proceedings of the Second BWEA Wind Energy Workshop,* Cranfield, England, Multi-Science, London, April 1980.

[15]Healey, J.V., "Tandem-Disk Theory—With Particular Reference to Vertical Axis Wind Turbines," *Journal of Energy,* Vol. 5, July-Aug. 1981, pp. 251–254.

[16]Paraschivoiu, I., "Double-Multiple Streamtube Model for Darrieus Wind Turbines," NASA CP 2185, May 1981.

[17]Paraschivoiu, I., "Aerodynamic Loads and Rotor Performance for the Darrieus Wind Turbine," AIAA Paper 81-2582, Dec. 1981.

[18]McCoy, H. and Loth, J.L., "Up- and Down-Wind Rotor Half Interference Model for VAWT," AIAA Paper 81-2579, Dec. 1981.

[19]Berg, D.E., "An Improved Double-Multiple Streamtube Model for the Darrieus-Type Vertical Axis Wind Turbine," *Proceedings of the Sixth Biennial Wind Energy Conference and Workshop,* Minneapolis, MN, June 1985, pp. 231–238.

[20]Paraschivoiu, I. and Delclaux, F., "Double-Multiple Streamtube Model with Recent Improvements," *Journal of Energy,* Vol. 7, May-June 1983, pp. 250–255.

[21]Paraschivoiu, I., Fraunie, P., and Beguier, C., "Streamtube Expansion Effects on the Darrieus Wind Turbine," *Journal of Propulsion and Power,* Vol. 1, March-April 1985, pp. 150–155.

[22]Strickland, J.H., Webster, B.T., and Nguyen, T., "A Vortex Model of the Darrieus Turbine: An Analytical and Experimental Study," *Journal of Fluids Engineering,* Vol. 101, Dec. 1979, pp. 500–505.

[23]Strickland, J.H., "A Vortex Model of the Darrieus Turbine: An Analytical and Experimental Study," Sandia National Laboratories, Albuquerque, NM, SAND79-7058, Feb. 1980.

[24]Strickland, J.H., Smith, T., and Sun, K., "A Vortex Model of the Darrieus Turbine: An Analytical and Experimental Study," Sandia National Laboratories, Albuquerque, NM, SAND81-7017, June 1981.

[25]Wilson, R.E. and Walker, S.N., "Fixed-Wake Analysis of the Darrieus Rotor," Sandia National Laboratories, Albuquerque, NM, SAND81-7026, July 1981.

[26]Milne-Thomson, L.M., *Theoretical Aerodynamics,* 2nd ed., Macmillan, 1952, pp. 246–253.

[27]Karamcheti, K., *Principles of Ideal-Fluid Aerodynamics,* Wiley, 1966, pp. 528–530.

[28]Fanucci, J.B. and Walters, R.E., "Innovative Wind Machines: The Theoretical Performances of a Vertical Axis Wind Turbine,"

Proceedings of the Vertical Axis Wind Turbine Technology Workshop, Sandia National Laboratories, Albuquerque, NM, SAND76-5586, May 1976, pp. III-61 to III-93.

[29]Currie, I.G., *Fundamental Mechanics of Fluids,* McGraw-Hill, 1974, pp. 50–52.

[30]Holme, O., "A Contribution to the Aerodynamic Theory of the Vertical Axis Wind Turbine," *Proceedings of the International Symposium on Wind Energy Systems,* St. John's College, Cambridge, England, Sept. 1976, pp. c4-55 – c4-72.

[31]Wilson, R.E., "Vortex Sheet Analysis of the Giromill," *Journal of Fluids Engineering,* Vol. 100, No. 3, Sept. 1978, pp. 340–342.

[32]Larsen, H.C., "Summary of a Vortex Theory for the Cyclogiro," *Proceedings of the Second U.S. National Conference on Wind Engineering Research,* Colorado State University, June 1975, pp. V-8, pp. 1-3.

[33]Sharpe, D.J., "A Vortex Flow Model for the Vertical Axis Wind Turbine," *Proceedings of the First British Wind Energy Association Wind Energy Workshop,* Multi-Science, London, April 1979, pp. 125–133.

[34]Azuma, A. and Kimura, S., "A Method of Calculation on the Airloading of Vertical-Axis Wind Turbines," *Proceedings of the 18th Intersociety Energy Conversion Engineering Conference,* Orlando, FL, Aug. 1983.

[35]Masse, B., "A Local-Circulation Model for Darrieus Vertical-Axis Wind Turbines," *Journal of Propulsion and Power,* Vol. 2, March-April 1986, pp. 135–141.

[36]Sheldahl, R.E. and Klimas, P.C., "Aerodynamic Characteristics of Several Symmetrical Airfoil Sections Through 180-Degree Angle of Attack for Use in Aerodynamic Analysis of Vertical Axis Wind Turbines," Sandia National Laboratories, Albuquerque, NM, SAND80-2114, March 1981.

[37]Eppler, R. and Somers, D., "A Computer Program for the Design and Analysis of Low-Speed Airfoils," NASA TM-80210, 1980.

[38]Migliore, P.G., Wolfe, W.P., and Fanucci, J.B., "Flow Curvature Effects on Darrieus Turbine Blade Aerodynamics," *Journal of Energy,* Vol. 4, March-April 1980, pp. 49–55.

[39]Klimas, P.C., "Vertical Axis Wind Turbine Aerodynamic Performance Prediction Methods," *Proceedings of the Vertical Axis Wind Turbine Design Technology Seminar for Industry,* Sandia National Laboratories, Albuquerque, NM, SAND80-0984, Aug. 1980.

[40]Berg, D.E., "Recent Improvements to the VDARTS VAWT Code," *Proceedings of the 1983 Wind and Solar Energy Technology Conference,* Kansas City, MO, April 1983, pp. 31–41.

[41]Gormont, R.E., "A Mathematical Model of Unsteady Aerodynamics and Radial Flow for Application to Helicopter Rotors," U.S. Army Air Mobility R&D Laboratory Report on Boeing-Vertol Contract DAAJ02-71-c-0045, May 1973.

[42]Noll, R.B. and Ham, N.D., "Effects of Dynamic Stall on SWECS," *Journal of Solar Energy Engineering,* Vol. 104, No. 2, May 1982, p. 96.

[43]Oler, J.W., Strickland, J.H., Im, B.J., and Graham, G.H., "Dynamic Stall Regulation of the Darrieus Turbine," Sandia National Laboratories, Albuquerque, NM, SAND83-7029, Aug. 1983.

[44]Worstell, M.H., "Aerodynamic Performance of the 17-m-diameter Darrieus Wind Turbine," Sandia National Laboratories, Albuquerque, NM, SAND78-1737, Jan. 1979.

[45]Reuter, R.C. Jr., "Tower Analysis," Sandia National Laboratories, Albuquerque, NM, SAND76-5586, May 1976, pp. 151–167.

[46]Rodeman, R., "Effects of System Imbalance," Sandia National Laboratories, Albuquerque, NM, SAND76-5586, May 1976, pp. 180–184.

[47]Lobitz, D.W. and Sullivan, W.N., "A Comparison of Finite Element Prediction and Experimental Data for Forced Response of DOE 100 kW VAWT," *Proceedings of the Sixth Biennial Wind Energy Conference and Workshop,* Minneapolis, MN, June 1983, pp. 843–853.

[48]Malcolm, D.J., "Structural Response of the DAF Indal 6400 VAWT," *Proceedings of Fourth ASME Wind Energy Symposium,* Dallas, TX, Feb. 1985, pp. 13–22.

[49]Popelka, D., "Aeroelastic Stability Analysis of the Darrieus Wind Turbine," Sandia National Laboratories, Albuquerque, NM, SAND82-0672, Feb. 1982.

[50]Lobitz, D.W. and Ashwill, T.D., "Aeroelastic Effects in the Structural Dynamic Analysis of Vertical Axis Wind Turbines," *Proceedings of Wind Power '85,* Aug. 1985, SERI/CP-217-2902, pp. 82–88.

[51]Lobitz, D.W., "Dynamic Analysis of Darrieus Vertical Axis Wind Turbine Rotors," Sandia National Laboratories, Albuquerque, NM, SAND80-2820, May 1981.

[52]Carne, T.G., "Finite Element Analysis and Model Testing of a Rotating Wind Turbine," Sandia National Laboratories, Albuquerque, NM, SAND82-0345, Oct. 1982.

[53]Veers, P.S., "Modeling Stochastic Wind Loads on Vertical-Axis Wind Turbines," Sandia National Laboratories, Albuquerque, NM, SAND83-1909, Sept. 1984.

[54]Lobitz, D.W., "Forced Vibration Analysis of Rotating Structures with Applications to VAWTs," *Proceedings of Fifth Biennial Wind Energy Conference and Workshop,* Vol. III, SERI/CP-635-1340, Oct. 1981, pp. 101–111.

[55]*MSC/NASTRAN User's Manual,* Vol. 2, McNeal-Schwendler Corp., Los Angeles, CA, 1981.

[56]Akins, R.E., "Performance Evaluation of Wind Energy Conversion Systems Using the Method of Bins-Current Status," Sandia National Laboratories, Albuquerque, NM, SAND77-1375, Feb. 1978.

[57]Akins, R.E., "Method of Bins Update," *Proceedings of Wind Energy Expo '82,* American Energy Association, Oct. 1982.

[58]Ashwill, T.D. and Leonard, T.M., "Development in Blade Shape Design for a Darrieus Vertical-Axis Wind Turbine," Sandia National Laboratories, Albuquerque, NM, SAND86-1085, Sept. 1986.

[59]Connell, J.R., "A Primer on Turbulence at the Wind Turbine Rotor," *Proceedings of Wind Power '85,* SERI/CP-217-2902, Aug. 1985, pp. 57–66.

[60]"Testing and Evaluation of a 500 kW Vertical-Axis Wind Turbine," Electric Power Research Institute, Palo Alto, CA, EPRI AP-4258, Sept. 1985.

[61]Kadlec, E.G., "The Potential of Advanced Darrieus Wind Turbines," *Proceedings of Sixth Biennial Wind Energy Conference and Workshop,* Minneapolis, MN, June 1983, pp. 213–218.

[62]Berg, D.E., "Structural Design of the Sandia 34-meter Vertical-Axis Wind Turbine," Sandia National Laboratories, Albuquerque, NM, SAND84-1287, April 1985.

[63]Banjannet, H., "Structural Design for a 4 MW VAWT—Project EOLE," INTERSOL '85 Biennial Congress of the International Solar Energy Society, Montreal, Quebec, Canada, June 1985.

[64]Kitada, T.A., Kaki, H.U., and Peters, L.K., "Estimation of Vertical Air Motion from Limited Horizontal Data: A Numerical Experiment," *Atmospheric Environment,* Vol. 17, 1983, pp. 2181–2192.

[65]Barnard, J.C., Wegley, H.L., and Hiester, T.R., "Improving the Performance of Mass-Consistent Numerical Models Using Optimization Techniques," Pacific Northwest Laboratory, Richland, WA, Rept. PNL-5566, Sept. 1985.

[66]Schatzle, P.R., Klimas, P.C., and Spahr, H.R., "Aerodynamic Interference Between Two Darrieus Wind Turbines," *Journal of Energy,* Vol. 5, March-April 1981, pp. 84–89.

[67]Marchetti, C. and Nakicenovic, N., "Market Penetration," *Energy in a Finite World,* 1979, pp. 253–279.

[68]Touryan, K.J., "The U.S. Solar Route," *Geopolitics of Energy,* Vol. 6, 1984, pp. 4–9.